Polymer/Trimer/Metal Complex Mixtures as Precursors of Gold Nanoparticles: Tuning the Morphology in the Solid-State

Carlos Díaz Valenzuela, Gabino A. Carriedo, M. Luisa Valenzuela, Luis Zúñiga, and Colm O'Dwyer

Abstract The pyrolysis of several physical mixtures of $AuCl(PPh_3)$ with polymeric $[NP(O_2C_{12}H_8)]_n$ or cyclic $N_3P_3(O_2C_{12}H_8)_3$ phosphazenes, formed as solid powders or films with different molar ratios, have been studied under air and at 800 °C. The characterization of the products has shown that the particle size and morphology are strongly dependent on the nature of the phosphazene, the phosphazene/$AuCl(PPh_3)$ molar ratio and on the preparation methodology. Gold nanoparticles (NPs) with mean sizes as small as 3.5 nm were obtained from a $[NP(O_2C_{12}H_8)]_n$/$AuCl(PPh_3)$ 1:1 film. The particle morphology was also strongly dependent on the experimentally conditions of the pyrolysis. Powdered materials exhibit a 3-D irregular morphology in the mixture $[NP(O_2C_{12}H_8)]_n$/$AuCl(PPh_3)$ 3:1 film, and gold foams in the 1:1 ratio, both from the $[NP(O_2C_{12}H_8)]_n$/$AuCl(PPh_3)$ as well as $N_3P_3(O_2C_{12}H_8)_3$/$AuCl(PPh_3)$ mixtures. These results show for the first time the possibility of controlling morphology and size of gold particles obtained by solid-state reactions.

Keywords Gold nanoparticle · Phosphazenes · Solid-state

1 Introduction

Gold based metal-noble nanoparticles (NPs) have attracted considerable interest due to the potential applications in catalysis, biolabeling, and plasmonics [1–5]. Understanding the factors that control the particle shape, size distribution and morphology is a key to the design of materials with desired optical and surface properties. Conventionally gold NPs are made either by the Turkevich [5, 6] or Brust–Schiffrin [7] methods. These methods are solution based and only a few solid-state reactions resulting in gold NPs have been reported [5, 8–11]. Thus, gold NPs 3–10 nm in size have been formed by heating in the solid state precursors NPs obtained by the Brust method [8, 9]. Additionally, the Au NP size can be increased by raising the reaction temperature. A similar solid-state approximation resulting in 2 nm gold NPs has been reported by Zhong [10]. Monolayers of gold were encapsulated in alkanethiolates, following the Brust method, and after heating the products in toluene to 150 °C, or in the presence of molten TOABr (tetraoctylammonium bromide), NPs with sizes in the 2–5 nm could be obtained by varying the temperature. On the other hand, Oiu et al. [11] obtained 6–8 nm gold NPs trapped in solid glass materials by irradiating a solid mixture containing the silicate glasses and Au_2O_3.

Electronic supplementary material The online version of this article (doi:10.1007/s10904-011-9601-8) contains supplementary material, which is available to authorized users.

C. D. Valenzuela (&) · L. Zúñiga
Departamento de Química, Facultad de Química, Universidad de Chile, La Palmeras 3425, Nuñoa, Casilla 653, Santiago de Chile, Chile
e-mail: mlvalenzuela@unab.cl

G. A. Carriedo (&)
Departamento de Química Orgánica e Inorgánica, Facultad de Química, Universidad de Oviedo, C/Julián Clavería S/N, 33071 Oviedo, Spain

M. Luisa Valenzuela
Departamento de Ciencias Química, Facultad de Ciencias Exactas, Universidad Andres Bello, Av. Republica 275, Santiago, Chile

C. O'Dwyer
Department of Physics & Energy, and Materials & Surface Science Institute, University of Limerick, Limerick, Ireland

Polyphosphazenes are inorganic macromolecules with alternating –N=P–N=P– chains with two side groups linked to the phosphorus atoms, that have many practical and potential applications as polymeric materials [12, 13]. A particular type of phosphazenes are those containing cyclic k^5-dioxydiaryl groups in the repeating units (poly-spyro-phosphazenes) [14], such as (1) the trimer $N_3P_3(O_2C_{12}H_8)_3$ ($O_2C_{12}H_8$=2,2^0-dioxy-1,1^0-biphenyl) and the high molecular weight polymer (2) $[NP(O_2C_{12}H_8)_2]_n$ [15] (Scheme 1). Various spyrophosphazenes, both polymeric and cyclic have been used to support transition metal organometallic complexes through a variety of attached ligands [12–14, 16–24] and recently polymers containing AuCl or $Au^?$ cations coordinated to the pendant phosphines present as O–C_6H_4–PPh_2 substituents have been described [25].

We have previously reported [26, 27] the preparation of Au nanostructured materials by pyrolysis of organometallic derivatives of cyclotriphosphazenes or polyphosphazenes under air at 800 °C. Thus, using the polymer $[\{NP(O_2C_{12}H_8)\}_{0.85}\{NP(OC_6H_5PPh_2–AuCl)_2\}_{0.15}]_n$ Au NPs with sizes in the range 90–130 nm were obtained [26]. On the other hand, using the polymer $[\{NP(O_2C_{12}H_8)\}_{0.7}\{NP(OC_5H_4N–4\{Au(C_6F_5)_2\}_{0.3}]_n$ as precursor, a 3-D network of porous Au was obtained [27].

The first step in the formation of such pyrolytic residues involves the cross-linking of the polymeric chain by the organometallic fragment. As pointed out by Allcock [12] cross-linking of the polymeric chain during the pyrolysis is a crucial step in the formation of ultrastructured materials by pyrolysis of polyphosphazenes.

In all the previous thermolytic studies, the organometallic metal–ligand fragments were covalently linked to the polymeric chain. Therefore, we considered of interest to compare the results with the thermolysis of related systems composed of similar polymers and complexes but intimately mixed in the solid state. We have performed analogous pyrolytic experiments of physical mixtures of organometallic complexes and polymers to study the pyrolytic products. In this work we describe the preparation of nanostructured gold particles of different size and shape by pyrolysis of mixtures of $AuCl(PPh)_3$ and the phosphazenes 1 (cyclic trimer) or 2 (polymer) (Scheme 1), in different molar ratios, prepared as precipitated powders or films.

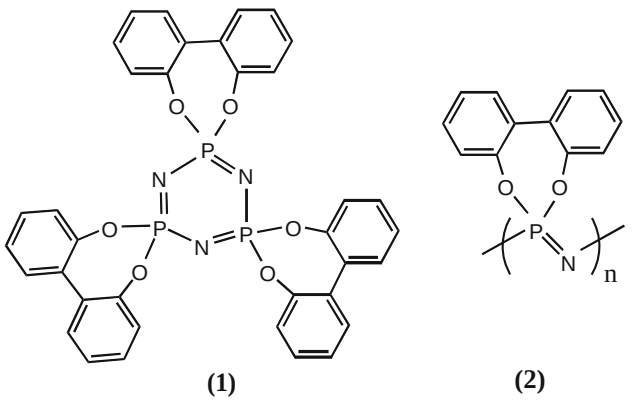

(1) **(2)**

Scheme 1 Formulas of the spyrocyclic triphosphazene (1) and the polyspyrophosphazene (2) component of the mixtures

2 Experimental

Solvents used were dried and purified using standard procedures. The starting materials $[NP(O_2C_{12}H_8)]_n$ [15] (with a Mw of 600,000) and $N_3P_3(O_2C_{12}H_8)_3$ [15] were prepared using the reported methods. The well known complex $AuCl(PPh_3)$ was prepared in high yield by adding AuCl (Aldrich) to a dichloromethane solution of PPh_3 (1:1 in moles) and evaporating the solvent. To the resulting white paste *n*-hexane was added and the white precipitate dried under vacuum for 3 h. Yield 96%. The purity of the product was checked and verified by ^{31}P-NMR.

X-ray diffraction (XRD) was carried out at room temperature on a Siemens D-5000 diffractometer in *h*–2*h* geometry. The XRD data was collected using Cu K*a* radiation (40 kV and 30 mA). Scanning electron microscopy (SEM) and energy dispersive X-ray analysis (EDX) were acquired with a JEOL 5410 SEM with a NORAN Instrument micro-probe transmission microscope and with a Hitachi SU-70 FESEM operating at 10 kV equipped with an Oxford Instrument X-max 50 mm^2 solid-state EDX detector. TEM images were made on a JEOL SX100 transmission microscope. The finely powered samples were dispersed in isopropanol and dropped on a conventional carbon-coated copper grid. AFM measurements were obtained using a Veeco Enviroscope in contact mode.

3 Preparation of the Mixtures

For the specific conditions see Table 1.

3.1 $[NP(O_2C_{12}H_8)]_n$/$AuCl(PPh_3)$

3.1.1 Film

A CH_2Cl_2 solution of the respective mixtures of $AuCl(PPh_3)$ and the trimer (1) or polymer (2) was allowed to evaporate slowly to cast a film that was dried at room temperature.

3.1.2 Powder (I)

The respective molar mixture of $AuCl(PPh_3)$ and the cyclotriphosphazene or polyphosphazene was dissolved in dichloromethane stirred for 24 h and evaporated until dry in a vacuum at 70 °C.

Table 1 Summary of the experimental conditions for the preparation of the mixtures $[NP(O_2C_{12}H_8)]_n/AuCl(PPh_3)$; n = 3 or polymer

Mixture	Polymer/Au	Trimer/Au	Mass of Au (g)	Mass of trimer (g)	Mass of polymer (g)
1a	1/1[a]		0.065		0.20
2a	3/1[a]		0.110		0.1538
1b	1/1[b]		0.065		0.20
2b	3/1[b]		0.110		0.153
1c	1/1[c]		0.12		0.055
2c	3/1[c]		0.091		0.126
3c	5/1[c]		0.110		0.254
1^0c		1/1[c]	0.0973	0.1351	
2^0c		3/1[c]	0.004	0.017	
3^0c		5/1[c]	0.0858	0.0238	
4^0c		10/1[c]	0.027	0.3865	

See Sect. 2

[a] Film

[b] Power method I

[c] Power method II

3.1.3 *Powder (II)*

The respective molar mixture of $AuCl(PPh_3)$ and the respective trimer or polymer was dissolved in THF, stirred for 24 h and evaporated until dry in a vacuum at room temperature.

3.2 $N_3P_3(O_2C_{12}H_8)_3/AuCl(PPh_3)$

These mixtures were prepared using the products described for the film and powders above. Experimental details for mixtures are summarized in Table 1.

4 Pyrolysis of the Mixtures

The pyrolysis experiments were made by pouring a weighed portion (0.05–0.15 g) of the respective mixtures 1a–c, 2a–c, 1^0c, 2^0c, 3^0c and 4^0c into aluminum oxide boats that were placed in a box furnace (Daihan oven model FHP-12) heating from 25 to 300 °C and then to 800 °C, and annealing for 2 h. The heating rate was maintained at 10 °C/min.

5 Results and Discussion

5.1 Pyrolytic Products from the $[NP(O_2C_{12}H_8)]_n/AuCl(PPh_3)$ Mixtures

From the pyrolysis of the 1:1 mixture of $[NP(O_2C_{12}H_8)]_n$ and $AuCl(PPh_3)$ (mixture 1c) (see Table 1), a yellow–orange material was obtained in 15% yield. The XRD patterns shown in Fig. 1a, exhibit the four (111), (200), (220), and (311) crystal reflections that can be indexed as the cubic fcc Au (PDF: 4-784) [26, 27]. The $I_{(220)}/I_{(111)}$ ratio was higher than observed for Au bulk (0.32) indicating a slightly enlarged (110) plane [28, 29]. Consistently, the EDAX analysis (Fig. 1b) exhibited only the presence of gold. As seen by SEM, the morphology of the material (Fig. 1c, d) is that of porous 2-D foam.

Metal foams are a relatively new class of materials with unique combinations of properties such as high stiffness, low density, gas permeability and thermal conductivity [30–36]. As such these materials promise to enable new technologies in areas as diverse as catalysis, fuel cells, hydrogen storage and thermal and acoustical insulation. Preparative methods for making metal foams to date have been somewhat limited in scope, with de-alloying of the bimetallic $Au_{022}Ag_{0.58}$ [33, 34] being the most commonly used. Similar metal foam materials were obtained from the pyrolysis of the polymer $\{[NP(O_2C_{12}H_8)]_{0.85}[NPOC_6H_4PPh_2{\cdot}AuCl]_{0.15}\}_n$ [26]. This relatively simple solid-state method allows access to unprecedented nanostructured monolithic noble metal foams using polyphosphazene templates.

In contrast to the formation of Au NPs from pyrolysis of the organo-gold containing polymer $\{[NP(O_2C_{12}H_8)]_{0.85}[NPOC_6H_4PPh_2{\cdot}AuCl]_{0.15}\}_n$ [26], no discrete nanosized Au structures were noted by TEM in the pyrolytic residue of mixture (1c). This suggests that under these conditions, the NPs are fused together in bulk crystals [34, 35]. The pyrolytic residues of the $[NP(O_2C_{12}H_8)]_n/AuCl(PPh_3)$ mixtures with molar ratios from 3:1 to 5:1 (2c), (3c) respectively, also consisted on cubic Au with foam-like morphologies (see Supplementary Material S1).

The procedure employed to prepare the mixtures also influenced the nature of the pyrolytic products. Thus, the 1:1 mixture $[NP(O_2C_{12}H_8)]_n/AuCl(PPh_3)$ obtained as a film using procedure 1 (mixture (1a)) and as powder using procedure 2 (mixture (1b)), resulted in the formation of cubic fcc Au in both cases after pyrolysis. The TEM images (Fig. 2a, b) however, evidenced that the mean sizes were different (3.5 and 75 nm respectively).

In agreement with the SEM and TEM observations, the AFM measurements conducted on these two deposits (see Supplementary Materials, S2) shows separate grain formation in both cases but with different size distribution. Thus this suggests that the support where the mixture is deposited and pyrolyzed influence the size and morphology.

The mixtures in 3:1 ratio (mixtures 2a and 2b), prepared as film and powders (using method 2) also formed cubic Au with similar dense grain morphology (Supplementary Materials, S3). The data suggest that there is not a

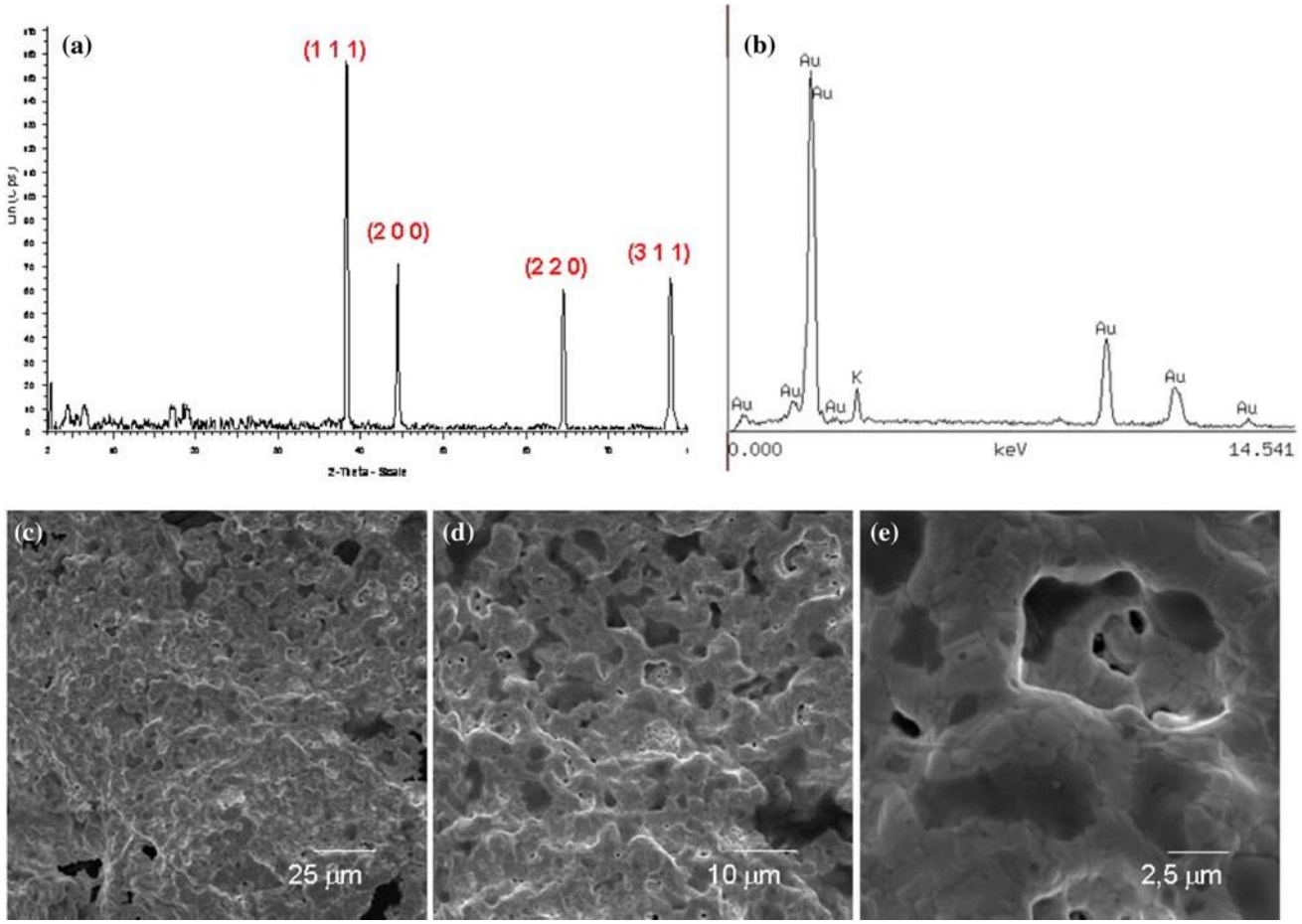

Fig. 1 XRD (a), EDS (b) and SEM images taken at several magnifications, (c), (d) and (e) of the pyrolytic product from the powder mixture

single, clear and general relationship between the $[NP(O_2C_{12}H_8)]_n$/$AuCl(PPh_3)$ ratio and the particle size, but some insight is found from the observation that small sized particles are uniquely found in the equivalent ratio mixtures, i.e. 1:1 polymer/Au and in the film. Control of particle size will also depend on the polymeric dewetting mechanism, thickness uniformity of the deposit and uniformity of heating throughout the deposit.

5.2 Pyrolytic Products from $N_3P_3(O_2C_{12}H_8)_3$/$AuCl(PPh_3)$ Mixtures

Pyrolysis of $N_3P_3(O_2C_{12}H_8)_3$/$AuCl(PPh_3)$ mixtures in several molar ratios 1^0c, 2^0c, 3^0c and 4^0c (see Table 1) also resulted in cubic Au. The XRD pattern shown in Fig. 3a for (1^0c) exhibits clearly the four (111), (200), (220), and (311) crystal facets that can be indexed as the cubic fcc Au (PDF: 4-784) [26, 27]. Their SEM images exhibited metal foam morphology, as seen in Fig. 3b. In this figure, the marks X_A and X_B indicate representative zones where the EDS show the only presence of Au; the entire network in fact consisted of pure Au. Corresponding TEM analysis shown in Fig. 3c, acquired in dark field, show the characteristic NP formation where the particles are measured to have a mean size of 4.7 nm (Fig. 3d). Other mixtures 2^0c, 3^0c, 4^0c exhibit similar features, as summarized in Supporting Information S4.

As in other investigations on gold NPs [6], the particle sizes were found to depend on the ratio $N_3P_3(O_2C_{12}H_8)_3$/$AuCl(PPh_3)$. In these cases, contrary to what is observed in classical solution methods for the preparation of Au NPs [6], the average particle size decreased from 6.5 to 4.7 nm as the $N_3P_3(O_2C_{12}H_8)_3$/$AuCl(PPh_3)$ ratio decreased (trimer/Au ratio of 5:1 to 1:1, respectively). Other $N_3P_3(O_2C_{12}H_8)_3$/$AuCl(PPh_3)$ mixtures (2^0c) and (4^0c) also exhibit cubic Au formation after pyrolysis with similar morphologies observed (Supplementary Materials, S4). As mentioned above, the $N_3P_3(O_2C_{12}H_8)_3$/$AuCl(PPh_3)$ ratio of 1:1 resulted in the smallest mean particle size of 4.7 nm.

6 Possible Formation Mechanism

Although the formation mechanism of Au NPs has been widely studied and recently revised [37–41], the solid-state

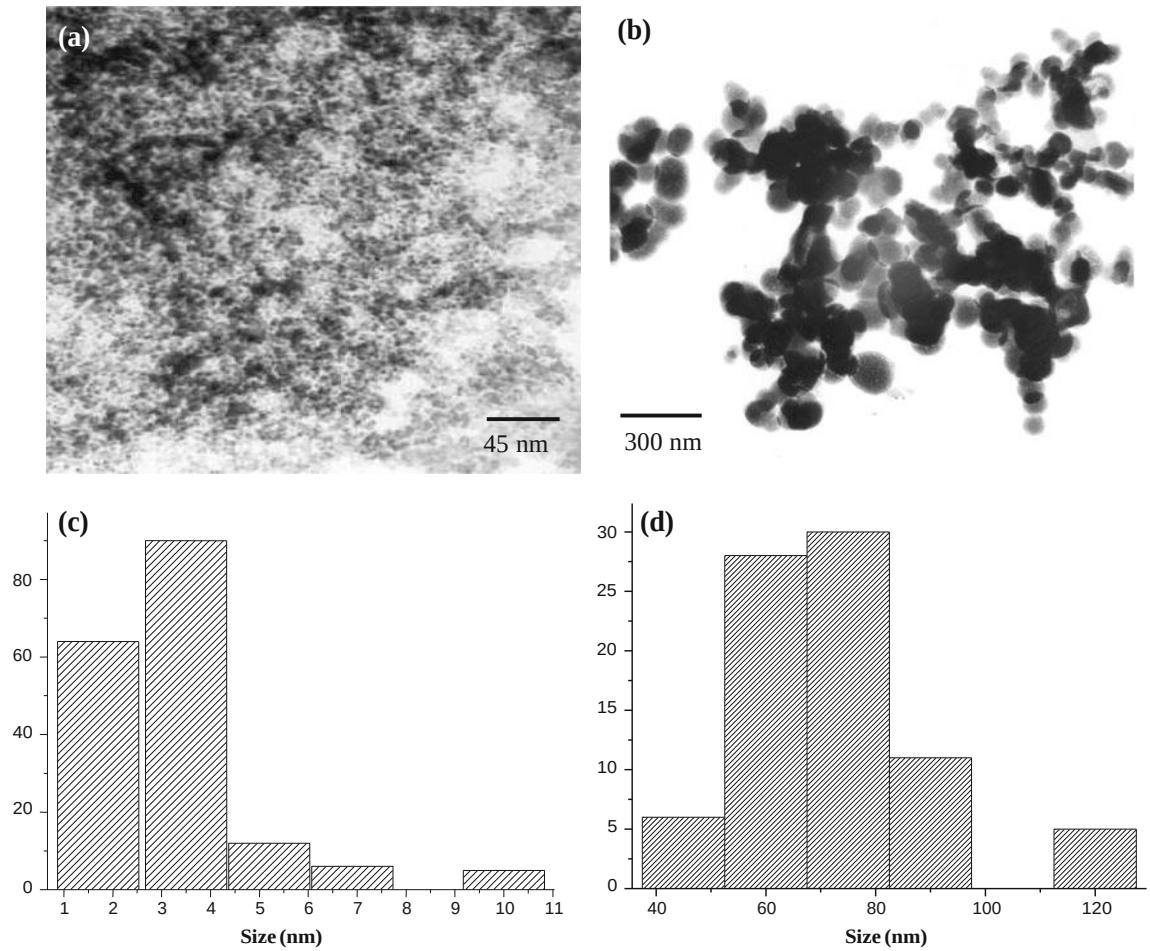

Fig. 2 TEM images of the pyrolytic product from film (a) and powder (b) Au/polymer 1:1 mixture and their respective size distribution histograms (c) and (d)

mechanism for the formation of Au NPs in solid-state [8–11] has not been significantly investigated or clarified [5]. The most probable mechanism of formation of Au nanostructures involve the energetically easy loss of Cl to give a $PPh_3Au^?$ species which is known to interact the *p* system of the aryl groups of the bispyro both of the polymer as well as the trimer [42–45]. These in turn afford a stable solid matrix which is not lost, as a volatile, in the first stage of the annealing. Subsequently oxidation of the organic matter gives rise to holes where the metallic gold begins to agglomerate, nucleate and grow. Sudden expulsion of gases (CO_2, NO_2 and other) produce in some cases metal foam products [31]. Some confirmation of this proposed mechanism stems from the TG/DSC measurements of the mixtures precursors. As is shown in Supplementary Materials (see S5), the TGA curve for the 1:1 mixture $N_3P_3(O_2C_{12}H_8)_3$/AuCl(PPh_3) exhibit a residue at 800 °C is 22.8% which compares well with calculated value of 21.69% corresponding to the gold content. The following main weight losses observed correspond to the calcination of the organic matter which can be separated for the two organic groups: the first two weight losses correspond to the $(O_2C_{12}H_8)_3$ groups, calculated as 45.57% and found to be 46.57% from the TGA data. The weight loss at 490 °C corresponds to the combustion of the Ph_3 groups, calculated 25.42% and the experimentally found to be 22.03%. In agreement with this, the DSC curve exhibits three exothermic peaks around 260 and 275 °C and one at 450 °C typical of the combustion of the organic matter [31]. A schematic model for the overall proposed mechanism is shown in Fig. 4.

Our previous solid-state approximation to Au nanostructured materials [26, 27] used the macromolecular Au-containing polymer having a uniform distribution of the Au(I) centers along the polymeric chains. This facilitated the migration of the Au atoms favoring the formation of nanoclusters and/or the 3D-network foam megastructures. In the case of the $N_3P_3(O_2C_{12}H_8)_3$/AuCl(PPh_3) and $[NP(O_2C_{12}H_8)]_n$/AuCl(PPh_3) mixtures, a strong Au–arene interaction between the $Au(PPh_3)^?$ cationic centers and biphenyl rings could permit a regular ordering of the Au centers along with the $NP(O_2C_{12}H_8)$ groups of the chains

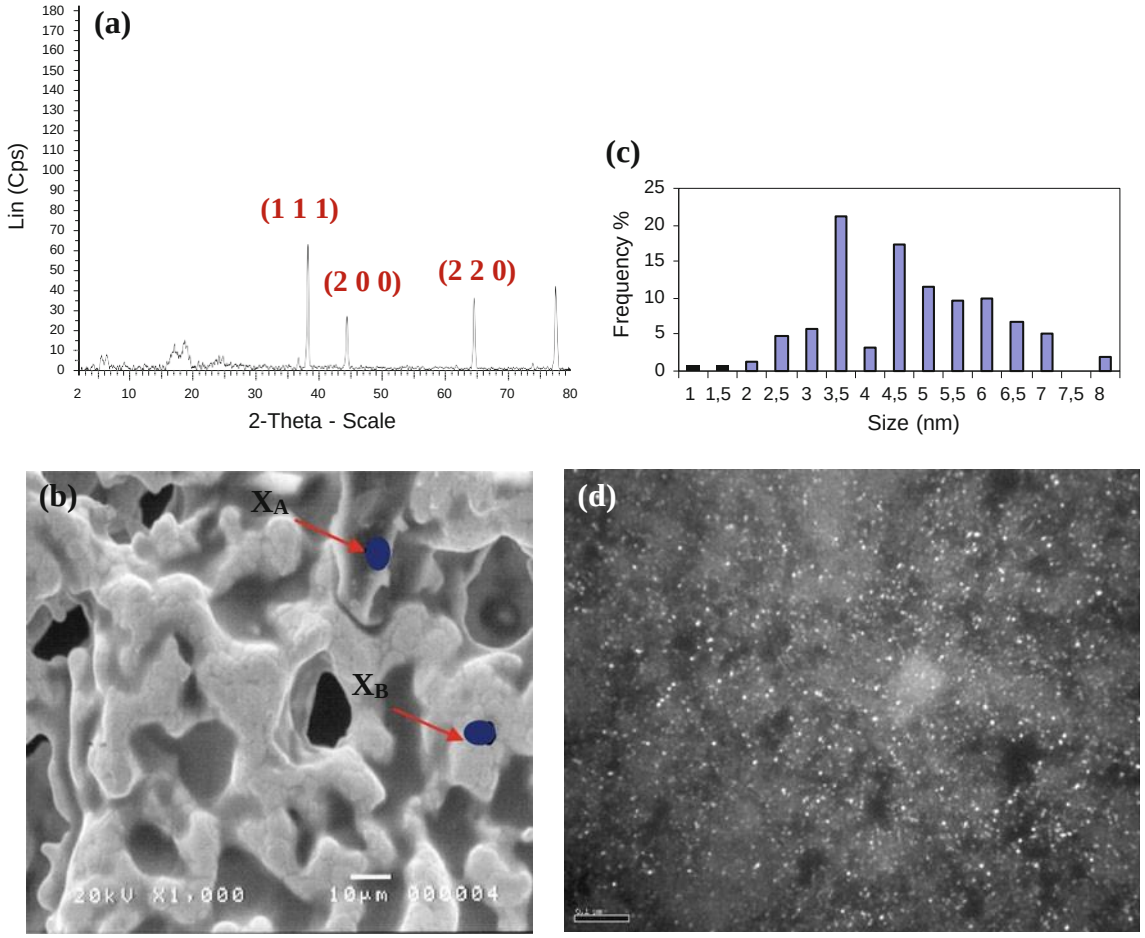

Fig. 3 a XRD spectrum, b SEM image, c dark field TEM image and d particle size histogram of the pyrolytic product (NPs) from mixture 1:1 $N_3P_3(O_2C_{12}H_8)_3$/AuCl(PPh_3) (1^0c)

of polymer 1 or around the cyclic molecules of the trimer 2. In Fig. 4 (top panel) a plausible general structure of the mixtures precursors is depicted.

Au(I)–arene interactions have been recently discussed by Laguna et al. [42–45]. Intermolecular gold-arenes have been reported in the trinuclear complex [Au_3(*p*-tolN=COEt)$_3$ [43]. Also metal–arene interactions have been observed in the one dimensional array supramolecular structures of the gold(I) complex [Au(CN){2,6-NC_5H_3(C_6H_4)$_2$–C,C^0N}] [44]. Intramolecular metal–arene interactions have been also observed in some complexes. Recently strong M–arene interactions (M = Au, Ag, Cu) have been reported in metal–dialkylbiarylphosphane complexes [45].

In comparison with our previous solid-state method for preparing metallic, metal oxide and metal phosphate NPs from organometallic derivatives of polyphosphazenes, the results presented here show that the formation of metallic nanostructures does not require the covalent linking of the organometallic fragment to the polymeric or trimeric phosphazenes structures. Thus the size of the Au NPs can be controlled by selecting the appropriate mixture for the precursor, e.g. $[NP(O_2C_{12}H_8)]_n$/AuCl(PPh_3) or $[NP(O_2C_{12}H_8)_3]$/AuCl(PPh_3) and an adequate preparation procedure. It is interesting to note that using this method, Au NPs as small as 3.5 nm can be obtained, with a mean size of $*5$ nm. As is known for gold, at ultra small NP sizes (typically $\backslash 2$ nm) quantum size effects start to be manifested. Such small sized NPs have thus far only been obtained using solution methods [46, 47]. As previously mentioned, Qiu et al. [11] have obtained solid Au NPs inside glasses with size in the range 6–8 nm. The main advantage of the preparation of solid Au NPs is that the NPs do not requires stabilizing molecules. In this method the presence of the $N_3P_3(O_2C_{12}H_8)_3$ or $N_3P_3(O_2C_{12}H_8)_n$ is crucial because solid-state pyrolysis of AuCl(PPh_3) results in bulk Au agglomerates (see Supporting Information S6).

The method described here allows the formation of small Au NPs, which to the best knowledge, are the smallest reported in large quantities synthesized entirely in solid-state. The ability to rationally prepare metallic and metal oxide NPs stems from the use of nanoscale metals

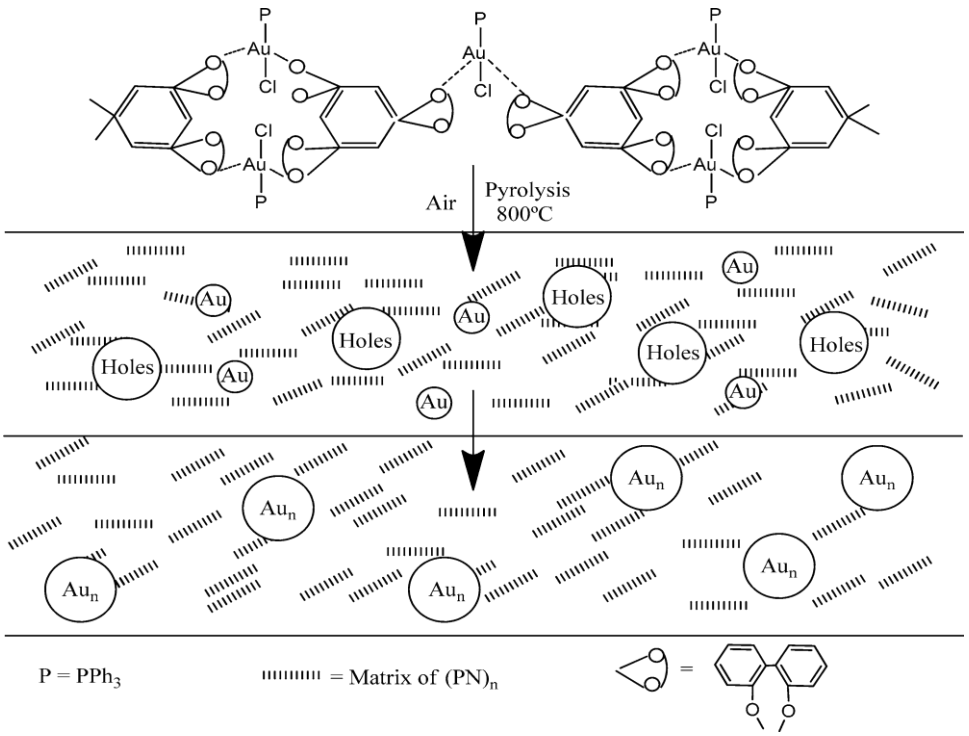

Fig. 4 Proposed mechanism $N_3P_3(O_2C_{12}H_8)_3$/AuCl(PPh_3) and $[NP(O_2C_{12}H_8)]_n$/AuCl(PPh_3) mixture as a precursor to nanostructured metallic materials

solid-state nanoelectronics and nanotechnology [48–50] and the need to deposit them through new routes. The principal problems for these requirements include mechanical and thermal stability of the nanoscale metals and also the limitations imposed by certain deposition methods for these metals. This method for preparing Au nanostructured materials completely in the solid-state is potentially useful in the fabrication of solid-state device contacts and interconnects in the field of electronics, as NP embedded materials for chemical sensing/detectors and catalysis, and also as surface plasmon-mediated sensors or support materials. Importantly, the method allows the deposition of metallic materials in the complete absence of water or liquids.

7 Conclusions

Metallic foams and NPs can now be easily prepared from mixtures of polymeric or cyclic phosphazenes and organometallic complexes containing the noble metal. For Au, we have shown that the variation of the phosphazene/Au ratios allows for the formation of either metallic foams of high density or discrete Au NPs, whose mean size and morphology are controlled through the structure of the precursor constituents and the relative ratio in the mixtures. With the $[NP(O_2C_{12}H_8)]_n$/AuCl(PPh_3) mixtures, Au NPs of 3.5 nm diameter were obtained from films formed through pyrolysis of the 1:1 mixture ratio, while with the analogous 1:1 mixture of $N_3P_3(O_2C_{12}H_8)_3$/AuCl(PPh_3) resulted in Au NPs with a mean diameter of 4.7 nm from a powder deposit. Comparison with previous studies shows that the formation of metallic nanostructures does not require the covalent linking of the organometallic fragment to the polymeric or trimeric phosphazenes, although the presence of the cyclic or polymeric phosphazene as solid-state template is necessary. The method allows the tuning of the resultant Au product; the Au is phase pure, single crystal and can be formed as small NPs or as low density, high surface area foams completely in the solid state.

Acknowledgments Financial support from Fondecyt (Project 1085011 and 1095135) and DGICYT (Project CTQ-2010-18330) is gratefully acknowledged.

References

1. M.-Ch. Daniel, D. Astruc, Chem. Rev. 104, 293–346 (2004)
2. J. Love, L.A. Estroff, J.K. Kriebel, R.G. Nuzzo, G.M. Whitesides, Chem. Rev. 105, 1103–1170 (2005)
3. A. Roncoux, J. Schulz, H. Patin, Chem. Rev. 102, 3757–3778 (2002)
4. G. Schmid, B. Corain, Eur. Inorg. Chem. 17, 3081–3098 (2003)
5. P.E. Chow, in *Gold Nanoparticles: Properties, Characterization and Fabrication*, Chap 14 (Nova Science Publishers, New York, 2010), pp. 307–314
6. J. Turkevich, P.C. Stevenson, J. Hillier, Discuss. Faraday Soc. 11, 55–75 (1951)
7. M. Brust, M. Walte, D. Berthell, D. Schiffrin, R. Whyman, J. Chem. Soc. Chem. Commun. 801–802 (1994)

8. T. Teranishi, S. Hasegawa, T. Shimizu, M. Miyake, Adv. Mater. 13, 1699–1701 (2001)
9. T. Shimizu, T. Teranishi, S. Hasegawa, M. Miyake, J. Phys. Chem. B. 107, 2719–2724 (2003)
10. M. Miyake, W. Zheng, F.L. Leibowitz, N.K. Ly, Ch. Zhong, Langmuir 16, 490–497 (2000)
11. J. Oiu, X. Jiang, C. Zhu, M. Shirai, J. Si, N. Jiang, K. Hirao, Angew. Chem. Int. Ed. 43, 2230–2234 (2004)
12. H.R. Allcock, Adv. Mater. 6, 106–115 (1994)
13. M. Gleria, R. De Jaeger, *Polyphosphazene: A Word Wide Insight* (Nova Science Publishers, New York, 2004)
14. G.A. Carriedo, J. Chil. Chem. Soc. 52, 119–195 (2007)
15. G.A. Carriedo, L. Fernández-Catuxo, F.J. García Alonso, P. Gómez-Elipe, P.A. González, Macromolecules 29, 5320–5325 (1996)
16. C. Díaz, M.L. Valenzuela, in *Horizons in Polymers Research*, Chapter 1, ed. R.K. Bregg (Nova Science Publishers, New York, 2005)
17. C. Díaz, P. Castillo, J. Inorg. Organomet. Polym. 11, 183–192 (2001)
18. C. Díaz, P. Castillo, G.A. Carriedo, P. Gómez-Elipe, F.J. García Alonso, Macromol. Chem. Phys. 203, 1912–1917 (2002)
19. C. Díaz, P. Castillo, Polym. Bull. 50, 183–192 (2003)
20. C. Díaz, M.L. Valenzuela, M. Barbosa, Mater. Res. Bull. 39, 9–19 (2004)
21. G.A. Carriedo, F.J. Garcia Alonso, P. Gómez-Elipe, C. Díaz, N. Yutronic, J. Chil. Chem. Soc. 48, 25–28 (2003)
22. G.A. Carriedo, F.J. García Alonso, C. Díaz, M.L. Valenzuela, Polyhedron 25, 105–112 (2006)
23. G.A. Carriedo, F.J. García Alonso, P. Gómez-Elipe, P.A. González, Polyhedron 18, 2853–2856 (1999)
24. G.A. Carriedo, F.J. García Alonso, P.A. González, C. Díaz, N. Yutronic, Polyhedron 21, 2579–2586 (2002)
25. G.A. Carriedo, F.J. García Alonso, J.L. García Álvarez, C. Díaz, N. Yutronic, Polyhedron 21, 2587–2592 (2002) (and references therein)
26. C. Díaz, M.L. Valenzuela, G.A. Carriedo, F.J. García Alonso, A. Presa, Polym. Bull. 57, 913–920 (2006)
27. J. Jiménez, A. Laguna, M. Benouazzane, J.A. Sanz, C. Díaz, M.L. Valenzuela, P.G. Jones, Chem. Eur. J. 15, 13509–13520 (2009)
28. Ch. Li, K.L. Shuford, Q.-H. Park, W. Cai, Y. Li, E.J. Lee, S.O. Cho, Angew. Chem. Int. Ed. 46, 3264–3268 (2007)
29. H.L. Wu, Ch. Kuo, M.H. Huang, Langmuir 26, 12307–12313 (2010)
30. A.M. Hodge, J.R. Hayes, J.A. Caro, J. Biener, A. Nhamza, Adv. Eng. Mater. 8, 853–857 (2006)
31. B.C. Tappan, M.H. Huyuh, M.A. Hiskey, D.E. Chavez, E.P. Luther, I.T. Mang, S.F. Son, J. Am. Chem. Soc. 128, 6589–6594 (2006)
32. I. Banhart, Adv. Eng. Mater. 8, 781–794 (2006)
33. H. Ehang, A.I. Cooper, J. Mater. Chem. 15, 2157–2159 (2005)
34. J. Biener, G.W. Nyce, A.M. Hodge, M.M. Biener, A.V. Hamza, S.A. Maier, Adv. Mater. 20, 1211–1217 (2008)
35. Y. Ding, J. Enlabacher, J. Am. Chem. Soc. 125, 7772–7773 (2003)
36. F. Khan, S. Mann, J. Phys. Chem. C 113, 19871–19874 (2009)
37. J.E. Millstone, S.J. Hurst, G.S. Metraux, J.I. Cutler, Ch.A. Mirkin, Small 5, 646–664 (2005)
38. L. Malfatti, D. Morongiu, S. Costacurta, P. Falcaro, H. Amenitsch, B. Marmiro, J. Li, G. Crenci, M.F. Casula, P. Innocenzi, Chem. Mater. 22, 2132–2137 (2010)
39. J. Polte, T.T. Ahner, F. Delissen, S. Sokolov, F. Emmerling, A.F. Thunemann, R. Kraehnert, J. Am. Chem. Soc. 132, 1296–1301 (2010)
40. X. Ji, X. Song, J. Li, Y. Bai, W. Yang, X. Peng, J. Am. Chem. Soc. 129, 13939–13948 (2007)
41. B.K. Pong, H.I. Elim, J.X. Chong, W. Ji, B.L. Trout, J.Y. Lee, J. Phys. Chem. C 111, 6281–6287 (2007)
42. A. Laguna, in *Modern Supramolecular Gold Chemistry*, Chapter 5 (Wiley WCH, Wenheim, 2008), p. 318
43. R.A. Rawashdeh-Omary, M.A. Omary, J.P. Fackler, R. Galassi, B.R. Pietroni, A. Burini, J. Am. Chem. Soc. 123, 9689–9691 (2001)
44. A.A. Mohamed, R.A. Rawashdeh-Omary, M.A. Omary, J.P. Fackler, Dalton Trans. 2597–2602 (2005)
45. P. Perez-Galan, N. Delpont, H. Guerrero-Gomez, F. Maseras, A.M. Echavarren, Chem. Eur. J. 16, 5324–5332 (2010)
46. M.J. Hostetler, J.E. Wingate, Ch.J. Zhong, J.E. Harris, E.W. Vachet, M.R. Clark, J.D. Londono, S.J. Green, J.J. Stokes, G.D. Wignall, G.L. Glish, M.D. Porter, N.D. Evans, R.W. Murray, Langmuir 14, 17–30 (1998)
47. P.D. Jadzinky, G. Calero, Ch.J. Ackerson, D.A. Bushnell, Ch.J. Kornberg, Science 318, 430–433 (2007)
48. G.B. Khomutov, V.V. Kislov, M.N. Antipirina, R.V. Gainutdinov, S.P. Gubin, A. Yy Obydenov, S.A. Pavlov, A.A. Rakhnyanskaya, A.N. Sergeev-Cherenkov, E.S. Soldatov, D.B. Suyatin, A.L. Toltikhina, A.S. Trifonov, T.V. Yurova, Microelectron. Eng. 69, 373–383 (2003)
49. G. Walters, I.P. Parkin, Chem. Mater. 19, 574–590 (2009)
50. E.C. Walker, K. Ng, M.P. Zach, R.M. Penner, F. Favier, Microelectron. Eng. 61, 555–561 (2002)